

One- dimensional numerical analysis for the porosity impact of open-cell metal foam on the effective thermal properties of PCMs

Farqad R Saeed¹, Natheer B Mahmood^{*2}, Marwah A Jasim³

¹ Ministry of science and technology/ Directorate of materials research /Baghdad

² Ministry of Education/General Directorate of Baghdad Education Karkh2/Iraq

³ University of Baghdad, College of Engineering, Iraq

ARTICLE INFO

Received: 3 June 2021;
Received in revised form:
28 Sept. 2021;
Accepted: 15 Oct. 2021;
Published online:
10 Nov. 2021

Keywords:

Phase change materials (PCMs)
Metal foam
Heat transfer rate
Melting front phase
Porosity

ABSTRACT

Metal foam has found its way in many engineering industries due to its ability to improve the heat transfer rate in thermal applications. Thermal energy storage based on phase change materials (PCMs) have significant importance as a part of renewable energy sources, and thermal management applications, However, low thermal conductivity is the essential drawback associated with the PCMs, especially the organic type of it, such as paraffin. Various experimental and numerical studies performed to test the effect of using metal foam with PCMs, in order to improve PCMs thermal conductivity. Many models suggested for evaluating the effective thermal conductivity of high porosity open cells metal foam, which immersed in base fluids of low thermal conductivity such as air, water, and PCMs. This work achieved numerically by using different models for calculating the effective thermal properties of metal foam with various range of porosities impregnate in paraffin. The study discussed the temperature distribution, which control the heat transfer rate, the behavior of temperatures versus time, and improvements in the melting front phase of the paraffin, under the effect of copper metal foam of various porosities and by applying different models, for estimating the effective thermal conductivity. The results exhibit an augmentation in the effective thermal conductivity with porosity decreasing. The outputs showed paradoxical results using the presented models and the differences between them have been discussed.

© Published at www.ijtf.org

1. Introduction

Improving the efficiency of energy systems became an essential demand associated with global development. Thermal energy storage (TES) based on PCMs received great attention as a part of the renewable

energy sources, on the other side the thermal management system based on PCMs such as the one used in the smart cars, both of them have been modified by using many ways to improve their efficiency.

*Corresponding e-mail: natheerbasheer@gmail.com (Natheer B. Mahmood)

The high thermal conductivity, and low

density, which can provide by the metal foam,

Nomenclature		Greek symbols	
a_1	Geometrical parameter controlling cross-sectional shape of ligament	α	Latent heat J/kg
C_p	Specific heat capacity, J/kgK	ε	Porosity
$C_{p,1}$	Specific heat capacity for the solid phase of the PCM, J/kgK	λ	Dimensionless parameter
$C_{p,2}$	Specific heat capacity for the liquid phase of the PCM, J/kgK	ρ	Density kg/m ³
d	Dimensionless foam ligament radius	ρ_1	Density of the solid phase of PCM kg/m ³
e	Dimensionless cubic node length	ρ_2	Density of the liquid phase of PCM kg/m ³
k_1	Thermal conductivity for the solid phase of the PCM, W/mK	ϕ	Volume fraction
k_2	Thermal conductivity for the liquid phase of the PCM, W/mK	ϕ_1	Volume fraction of the solid phase of PCM
k_{eff}	Effective thermal conductivity of the metal foam/PCM, W/mK	ϕ_2	Volume fraction of the liquid phase of PCM
k_f	Thermal conductivity for the PCM, W/mK	Subscripts	
k_s	Thermal conductivity for the metal foam, W/mK	A	Unit cell subsection
R	Simplification quantity, mK/W	a	Layer a of unit cell
T	Temperature, K	B	Unit cell subsection
T_w	Temperature at the wall, K	b	Layer b of unit cell
T_m	Melting front temperature, K	C	Unit cell subsection
t	Time, s	c	Layer c of unit cell
x	System length, m	D	Unit cell subsection
		m	Melting phase

make it the concern of the researchers. According to the mentioned above metal foam applied in many applications including the TES [1,2], heat exchangers [3,4], and heat sinks [2], which impregnate in various types of fluids such as water and air or PCMs such as paraffin. The using of high porosity open cells metal foam immersed in PCMs to improve the heat transfer rate of the PCM proved its high performance [5,6]. The value of the effective thermal conductivity for the metal foam immersed in a specific fluid is a necessary characteristic to be counted for heat transfer applications [7]. Calmidi and Mahajan [8] designed a model for predicting the effective thermal conductivity of the metal foam/base fluid, which based on developing an empirical correlation and they derived a theoretical model based on a hexagonal pore shape. They found that their model agreed with experimental data with 10 % deviation when the area ratio ($2a/r$) fixed at 0.09. The model was developed by Bhattacharya *et al.* [9] which replaced the node shape from the cubic to the circular one. The result of their model that it is possible to have accurate outputs for high porosity metal foam by selecting a suitable ratio between the ligaments to the node radius. They also developed an empirical correlation for finding

the effective thermal conductivity as a function of porosity. A one-dimensional model for the effective thermal conductivity of the open-cell metal foam based on three-dimensional unit cell geometry suggested by Boomsma and Poulidakos [10]. Their result was that the effect of the solid phase on the overall effective thermal conductivity has a significant impact on it. Ligament orientation is an important factor that has been considered by Dai *et al.* [11], which they developed the model of Boomsma and Poulidakos to include the mentioned effect. Their results were more accurate for predicting the effective thermal conductivity of fluid/metal foam. It should be mentioned that all the previous models are based on empirical parameters exhibiting the geometrical relationship between the ligament and the node of the metal foam. The used models to predict the effective thermal conductivity is based on experimental data; on the other hand, aluminum metal foam generally used to extract the mentioned data. Accordingly, the validity of most correlation depends on these results. The effect of porosity on the metal foam thermal conductivity studied by Calmidi and Mahajan [12,8] and Phanikumar and Mahajan [13]. They indicated the effect of porosity on the thermal

conductivity of aluminum metal foam with a range of porosity size 0.9-0.98. Their experiment achieved by using water and air as a fluid. They found that thermal conductivity increased with decreasing the porosity. A transient photo-thermal method used by Fetoui *et al.* [14] to indicate the effective thermal conductivity for the aluminum metal foam and air. Their results were similar to the resemble experiments. The effective thermal conductivity for the Copper and Nikel foam impregnate with paraffin performed by Xiao *et al* [15,16], recorded a perfect improvement in the effective thermal conductivity especially by using the copper foam. The use of high porosity open-cell copper foam has great importance and requires a multi-study due to its demands in many applications [17,18]. The aim of this work is to study the effect of porosity on the heat transfer rate for copper metal foam saturated in paraffin numerically, by using different models to calculate the effective thermal conductivity for the composite of metal foam immersed in a specific fluid.

2. Mathematical Model

The dimensional governing equation, which describes the temperature distribution in the liquid phase, is [19]:

$$(\rho C_p) \frac{\partial T}{\partial t} = k \frac{\partial^2 T}{\partial x^2} \quad (1)$$

The boundary conditions Wall temperature $T(x=0, t > 0) = T_w$

Melting front temperature.

$$T(x=x(t), t > 0) = T_m$$

1D model has been applied in the present work to expose the case as simple as possible and explore the predicted results in this case. The effective thermal conductivity calculation for metal foam/PCM composite has been obtained using a special model, then substituting the resulted effective thermal conductivity of the mixture to the required governing equations and phase change equations dealing with the mixture as a single phase. This procedure has been followed by the present numerical work.

The equations, which control the phase change that happens in the PCMs and associated properties such as, thermal conductivity, thermal diffusivity, specific heat capacity, and density are [19]:

$$\rho = \rho_1 \phi_1 + \rho_2 \phi_2 \quad (2)$$

$$C_p = \frac{1}{\rho} (\rho_1 \phi_1 C_{p,1} + \rho_2 \phi_2 C_{p,2}) + L_{1 \rightarrow 2} \frac{\partial \alpha_m}{\partial T} \quad (3)$$

$$\alpha_m = \frac{1}{2} \frac{\rho_2 \phi_2 - \rho_1 \phi_1}{\rho_1 \phi_1 + \rho_2 \phi_2} \quad (4)$$

$$k = \phi_1 k_1 + \phi_2 k_2 \quad (5)$$

Effective thermal conductivity for the PCM/metal foam can be calculated through specific correlations, which used in the present work. The most essential models used by the researchers, applied in this study to explore their mechanisms and the differences between them.

2.1 Model one, for Calculating Effective Thermal Conductivity (k_{eff1})

The first model is suggested by Boomsma, and Poulikakos [10], which based on 3D tetrakaidecahedron shape and contain empirical parameters with respect to the filling medium. They skipped the ligament orientation effect, $e=0.339$.

$$R_A = \frac{4d}{(2e^2 + \pi d(1-e))k_s + (4 - 2e^2 - \pi d(1-e))k_f} \quad (6)$$

$$R_B = \frac{(e-2d)^2}{(e-2d)e^2k_s + (2e-4d - (e-2d)e^2)k_f} \quad (7)$$

$$R_C = \frac{(\sqrt{2}-2e)^2}{2\pi d^2(1-2e\sqrt{2})k_s + 2(\sqrt{2}-2e-\pi d^2(1-2e\sqrt{2}))k_f} \quad (8)$$

$$R_D = \frac{2e}{e^2k_s + (4-e^2)k_f} \quad (9)$$

$$k_{eff1} = \frac{\sqrt{2}}{2(R_A + R_B + R_C + R_D)} \quad (10)$$

2.2 Model two, for Calculating Effective Thermal Conductivity (k_{eff2})

This model is a development for the Boomsma and Poulikakos [10], that in the first model they skipped the ligament orientation impact, while in this model which presented by Dai *et al* [11] they included this effect according to the following correlation.

$$k_{eff2} = \varepsilon k_f + (1-\varepsilon)k_s \cos^2 \theta \quad (11)$$

This model obeys to the same conditions for the first one excluding the ligament orientation effect, which ignored in the first model.

2.3 Model three, for Calculating Effective Thermal Conductivity (k_{eff3})

This model presented by Yao et al. [20], the model based on 3D tetrakaidecahedron shape, No empirical parameters have been included in this model, also the model contains the ligament orientation effect $a=2.01$.

$$\varepsilon = 1 - \frac{\sqrt{2}}{2} \pi \lambda^2 (3-5\lambda) \frac{1+a_1^2}{a_1^2} \quad (12)$$

$$k_a = \frac{\sqrt{2}}{6} \pi \lambda (3-4\lambda) \frac{1+a_1^2}{a_1^2} k_s + \left[1 - \frac{\sqrt{2}}{6} \pi \lambda (3-4\lambda) \frac{1+a_1^2}{a_1^2} \right] k_f \quad (13)$$

$$k_b = \frac{\sqrt{2}}{2} \pi \lambda^2 \frac{1+a_1^2}{a_1^2} k_s + \left(1 - \frac{\sqrt{2}}{2} \pi \lambda^2 \frac{1+a_1^2}{a_1^2} \right) k_f \quad (14)$$

$$k_c = \frac{\sqrt{2}}{6} \pi \lambda^2 \frac{1+a_1^2}{a_1^2} k_s + \left(1 - \frac{\sqrt{2}}{6} \pi \lambda^2 \frac{1+a_1^2}{a_1^2} \right) k_f \quad (15)$$

$$k_{eff3} = \frac{1}{\left(\frac{\lambda}{k_a} \right) + \left(\frac{(1-2\lambda)}{k_b} \right) + \left(\frac{\lambda}{k_c} \right)} \quad (16)$$

In the presented work calculating the effective thermal conductivity of metal foam/PCM composite at various range of porosity, using specific models, then the results of the effective thermal conductivity are used to calculate the heat transfer along the x-axis considering the metal foam and PCM composite as a single phase. However, the space factor could have a direct effect on the presented results, but the present work focused on studying the case for the composite when it is supplied to a constant temperature source from one side and the development of temperature along the x-axis, specifically.

Regarding the ligament orientation, the calculating effective thermal conductivity of metal foam/PCM gives the most accurate results in case when the conduction in the fluid and conduction in the ligament are not aligned with each other. However, two cases have been studied taking into account the conduction in the fluid is aligned and not aligned with the ligament orientation as presented by Dai et al [11] and their outcomes ensure that including the ligament orientation predicate the effective thermal conductivity more accurate. According to the mentioned information, the model, which

includes the ligament orientation has been used in the present work.

3. Geometry of the numerical simulation

A one-dimensional geometry of 10 cm in length supplied to constant temperature 253 [K] from one side and the other side is thermally insulated as shown in Fig. 1. The maximum element size that used is 6.7 mm, the maximum element growth rate is 1.3, and the resolution of the narrow region is 1. The thermo-physical properties of the PCM (paraffin) are listed in Table. 1. The thermal conductivity of the used copper metal foam is 401 W/m.K, and the range of the porosity is 0.88 to 0.98. Fig. 2 Shows a rectangular unit inserted into one face of Tetradekahedron, as described by Boomsma and Poulikakos [10]. The finite element method is used to obtain the solution in the current work that this method is efficient and followed by many studies [21,22].

Table. 1.

Thermophysical properties for the paraffin.

Physical Property	Solid phase	Liquid Phase
Thermal conductivity	0.21 [W/m K]	0.21 [W/m K]
Specific heat capacity	1.62 [J/g.K]	1.68 [J/g.K]
Density	922.619 [kg/m ³]	780 [kg/m ³]
Latent heat	181 [kJ/kg]	181 [kJ/kg]
Melting temperature range	317.2 [K] to 324.9 [K]	317.2 [K] to 324.9 [K]

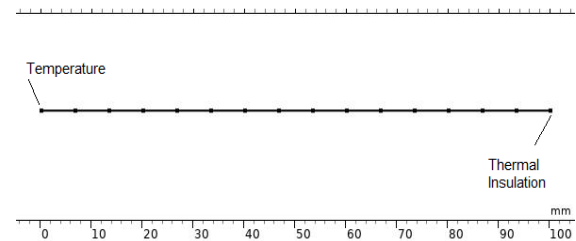


Fig. 1. Schematic representation of the used geometry.

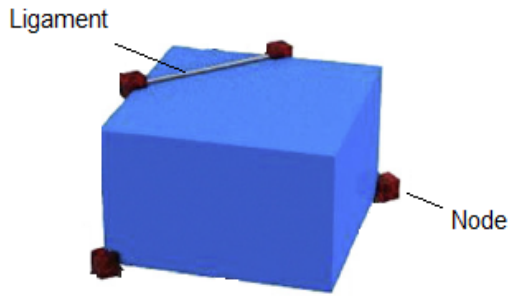


Fig. 2. Shows a rectangular unit inserted into one face of Tetradecahedron, as described by Boomsma and Poulidakos [10].

4. The validity

The validity of the present study obtained by indicating the temperature distribution along with the x-axis distance at different times in comparison with OGOH *et al.* work [19]. However, the followed work used a 2D semi-infinite system that the length of their system is four times, compared to the area affected by the temperature, which exhibits the 1D behavior along the centerline, While, the present work uses a 1D system directly. **Fig. 3 (a)** shows the temperature distribution along the x-axis (b) indicates the position of the melting front phase of paraffin, in comparison to the analytical and numerical work achieved by OGOH *et al.*, which exhibits a very close behavior to the presented work. The small variation among the behaviors can interpreted because of the 2D semi-infinite system suggested by OGOH *et al.* and the 1D system offered by this study.

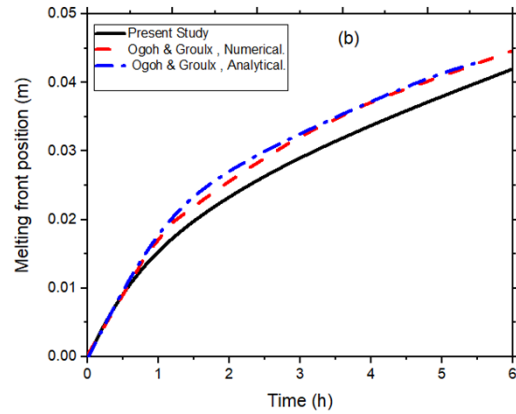
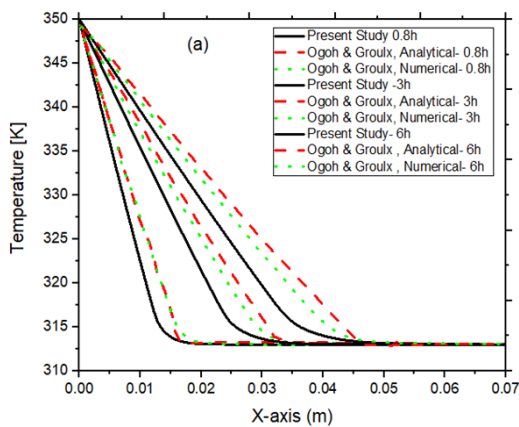


Fig. 3. (a): Shows the temperature distribution along the x-axis (b) Melting front position versus time, of the present study in comparison to the analytical and numerical work achieved by OGOH *et al.* [19].

5. Results and Discussion

5.1 Temperature distribution

Temperature distribution along the x-axis shown in **Figures 4-6**, which indicate the behavior of the temperature distribution using metal foam with different porosities in comparison to the pure paraffin. The general results indicated at all figures, and by applying different models mentioned earlier, a huge improvement in heat transfer rate and augmentation in temperatures distribution by using copper metal foam with the paraffin. On the other side, it can be noticed that the heat transfer rate enhanced with the decreasing of the porosity, that 0.88 porosity recorded the maximum improvement while the 0.98 porosity exhibited the minimum enhancement. The recordings at the porosities between 0.98 to 0.88 show a gradual increase in heat transfer reaching the maximum at 0.88 porosity. Three models used to indicate the mentioned results each one follows a specific mechanism. The first model performed by Boomsma and Poulidakos [10], which based on empirical parameters with no respect for the ligament orientation. The model indicated improvement in thermal distribution toward the x-axis at different times as shown in **Fig. 4**, the thermal distribution increased gradually with time from 300, 600, 900, reaching the maximum value at the 1200 s, which indicates the highest heat transfer rate as expected. The temperature distribution augmented with decreasing

porosity for all times. The modified model presented by Dai *et al* [11] included the ligament orientation effect to give higher improvement than the first model that temperature distribution along the x-axis gave higher recordings for all porosities and times as indicated in Fig. 5. Finally, the final model presented by Yao *et al.* [20] Fig. 6 which does not rely on empirical parameters and take into account the ligament orientation effect exhibit a mediator improvement lies in between Boomsma and Poulikakos [10], and Dai *et al.* [11]. The general behavior of the model resembles the other models that temperature distribution increased with time and by decreasing the porosity.

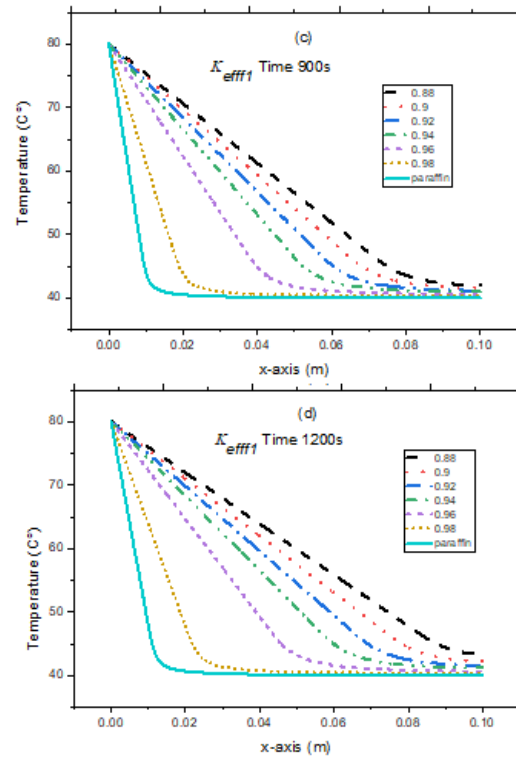
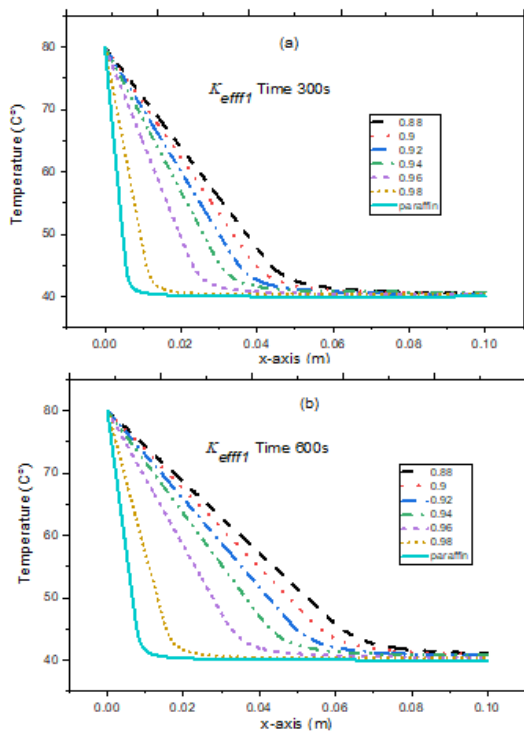
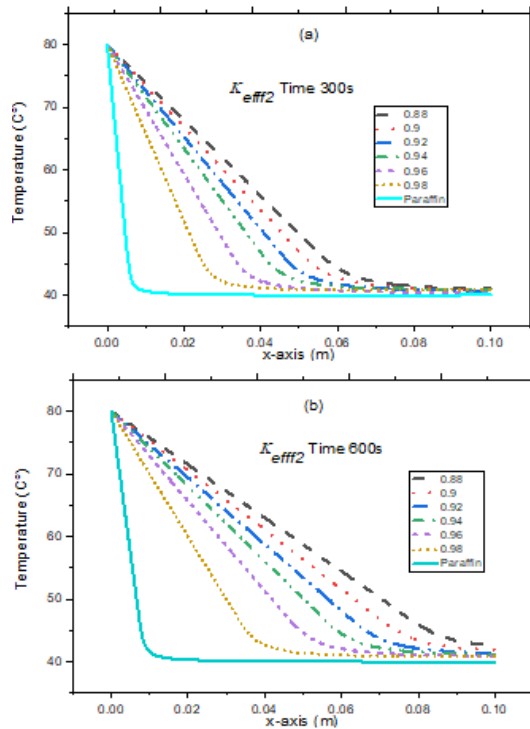


Fig. 4. Temperature distribution along the x-axis by using Boomsma and Poulikakos Model [10], (a) at 300 s, (b) at 600 s, (c) at 900 s, (d) at 1200 s.



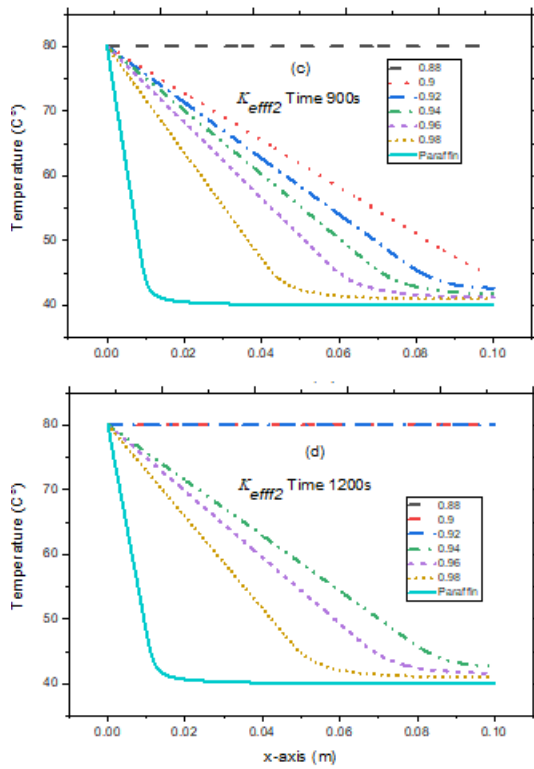


Fig. 5: Temperature distribution along the x-axis by using Dai *et al.* Model [11], (a) at 300 s, (b) at 600 s, (c) at 900 s, (d) at 1200 s.

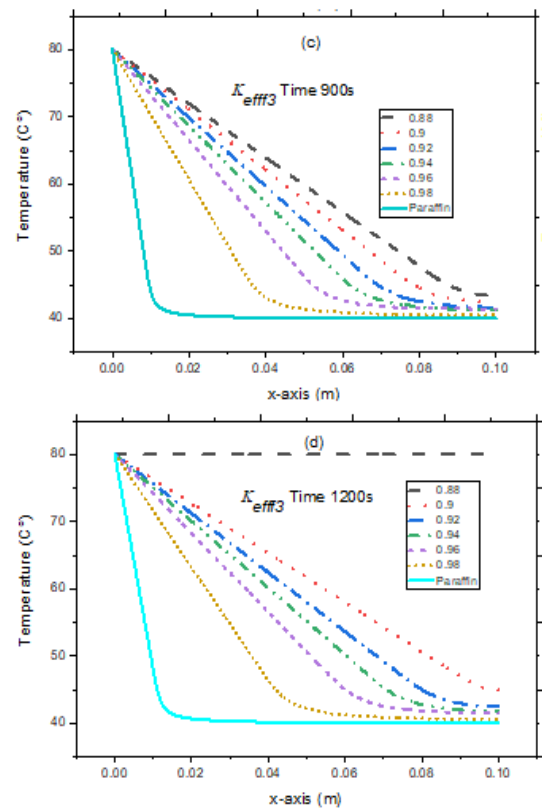
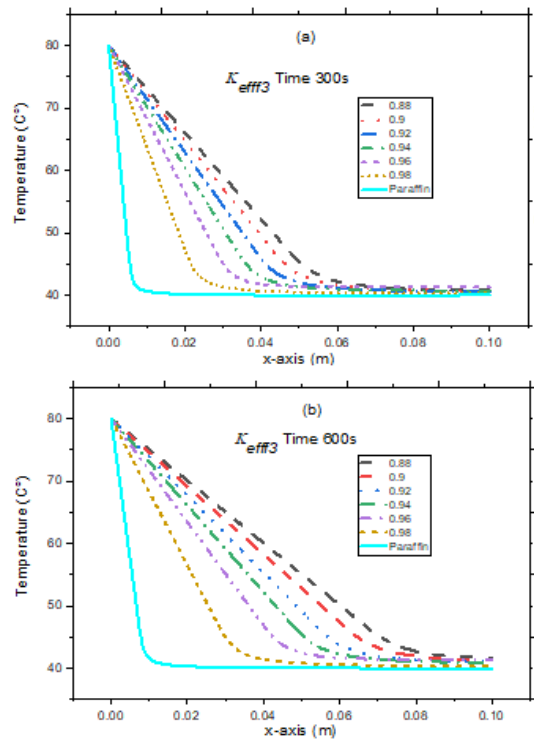


Fig. 6: Temperature distribution along the x-axis by using Yao *et al.* Model [20], (a) at 300 s, (b) at 600 s, (c) at 900 s, (d) at 1200 s.



5.2 The Temperature behavior versus time

The rising in temperature at specific points along the x-axis measured with time variation, where the temperature behavior detected at 1, 25, 50, 75 mm, respectively. A significant increase in temperature achieved by using the copper metal foam with paraffin in comparison to the pure paraffin. The general behavior of the curve is a rapid increase in temperature reaching the maximum value 80 °C at x=1 mm, at the closest point to the temperature source as noticed from **Figures 7 - 9** (a). On the other hand, the other **Figures 7 - 9** (b), (c), and (d). shows a gradual increase in temperature depending on the position of the indicated point. The rising in temperature is faster which can be interpreted by the following, whenever the indicated point is closer to the temperature source, the effect of sensible heat is more clear which associated with latent heat and it can notice in 0 to 1400 s at 0.88 porosity and x = 25 as shown in **Fig. 7** (a). The mentioned effect of the sensible heat vanished gradually on the

latent heat zone when the measured point gets far from the temperature source as shown in Fig.7 (d). Which offers the effect of latent heat until the 1400 s then a rapid change in temperature as a sensible heat. The temperature behavior versus time detected by using a range of porosities 0.88 to 0.98 at various distances as it mentioned and by applying different models to indicate the effective thermal conductivity. One can observe that increasing in temperature with time enhanced by decreasing the porosity as shown in Figures 7 - 9, however, a paradoxical improvement recorded by using the presented models. The first model presented by Boomsma, and Poulikakos [10], indicated the maximum raising in temperature 80°C, at 1400 s for 0.88 porosity and $x=25$ mm, while the maximum raising in temperature 80°C, at 1750 s for 0.9 porosity and $x=25$ mm. The other used porosities 0.92 to 0.98 does not reach the maximum temperature 80°C even after 2000 s (the whole time used for comparison) at $x=25$ mm. The explained behavior is the same at the all axis points $x=1, 25, 50, 75$ mm used in the simulation. The second model for Dai *et al* [11], exhibit a higher performance as a result for counting the effect of ligament orientation. The model recorded maximum temperature 80°C, at 800 s for 0.88 porosity and $x=25$ mm, while the maximum temperature 80°C found at 950, 1200, and 1600 s, for 0.9, 0.92, and 0.94 porosity and $x=25$ mm. The last model which completely based on theoretical parameters by Yao *et al.* [20], the outputs of the model lie in between the first and the second one. That maximum temperature 80°, at 1000 s for 0.88 porosity and $x=25$ mm, while the maximum temperatures 80°C, located at 1200, 1600, and 1850 s, for 0.9, 0.92, and 0.94 porosities and $x=25$ mm.

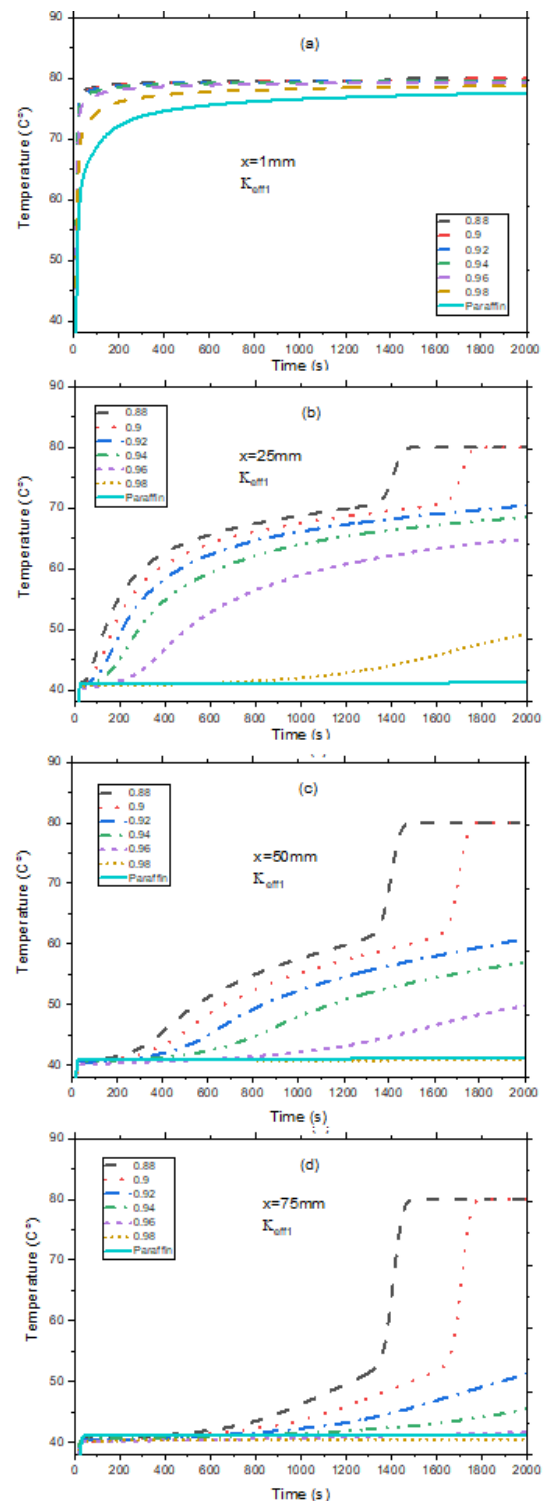


Fig. 7. Temperature versus time at specific points along the x -axis by using Boomsma, and Poulikakos Model [10], (a) $x=1$ mm, (b) $x=25$ mm, (c) $x=50$ mm, (d) $x=75$ mm.

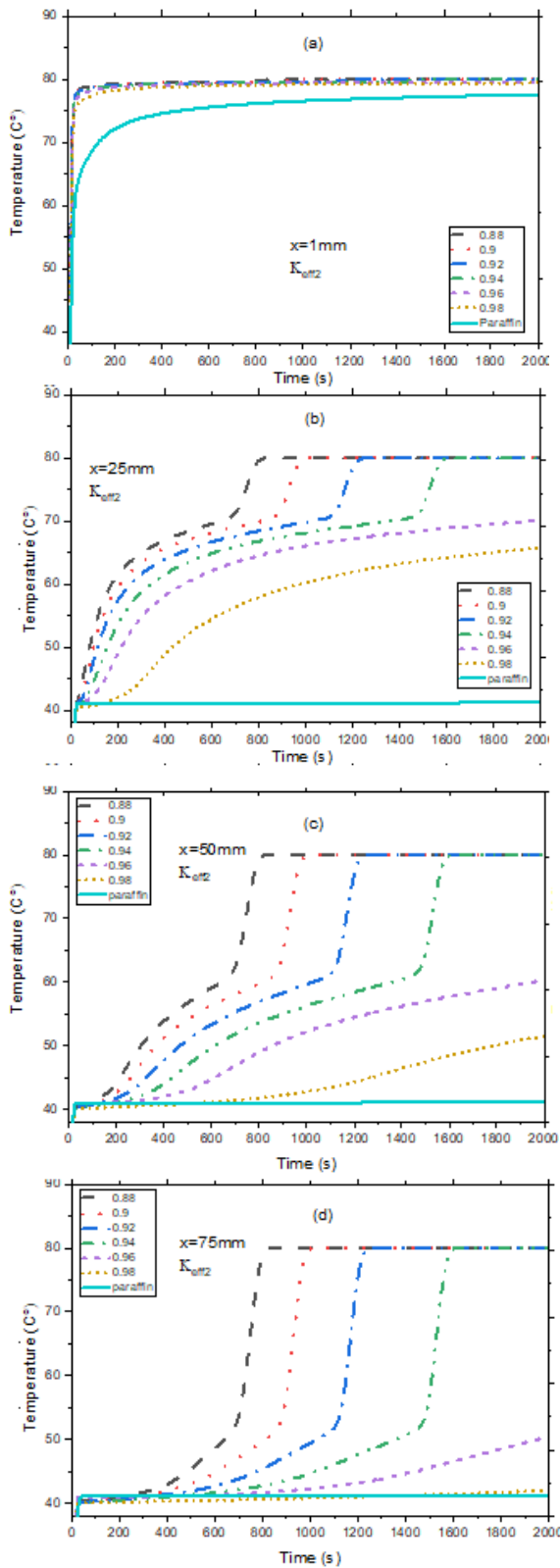


Fig.8. Temperature versus time at specific points along the x-axis by using Dai *et al.* Model [11], (a) $x=1$ mm, (b) $x=25$ mm, (c) $x=50$ mm, (d) $x=75$ mm.

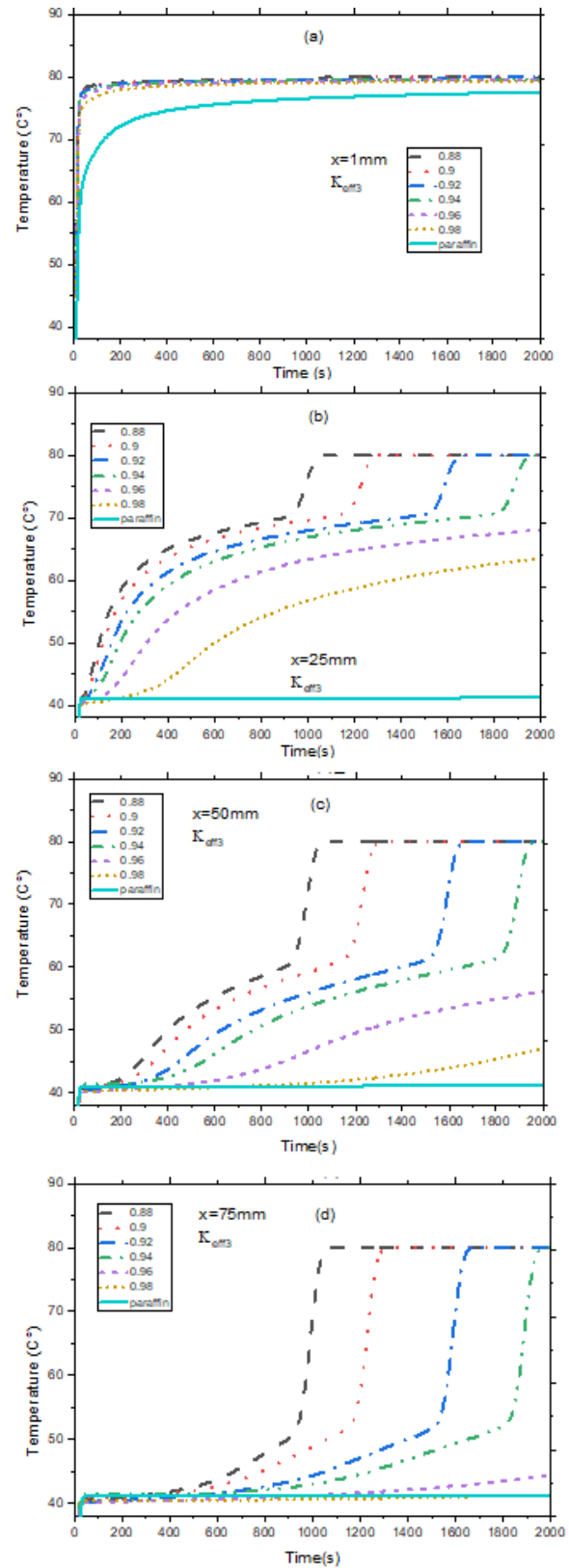


Fig. 9. Temperature versus time at specific points along the x-axis by using Yao *et al.* Model [20], (a) $x=1$ mm, (b) $x=25$ mm, (c) $x=50$ mm, (d) $x=75$ mm.

5.3 The effect of porosity on temperature differences (ΔT)

The temperature differences measured between two points $x=1\text{ mm}$, and $x=25\text{ mm}$, on the x -axis at various porosities. The ΔT indicated by using the three presented models to clarify the variation between each model in detecting the thermal distribution. The ΔT decreased with decreasing the porosity that the minimum recordings of ΔT found at 0.88 porosity and increased gradually with increasing the porosity, and maximum ΔT detected at 0.98 as shown in Fig. 10. The figures exhibit a variation in the results depending on the used models. The reduction in ΔT values can be arranged according to the applied model from maximum to minimum which are Dai et al. [11], Boomsma and Poulikakos [10], and Yao et al., respectively. The figures show the importance of selecting the optimum porosity in enhancing the heat transfer rate and improving the thermal distribution which decreases the ΔT along the x -axis. In addition, the previous results show the paradoxical behavior between the presented models in the detection of the effective thermal conductivities and its effect on the general thermal behavior.

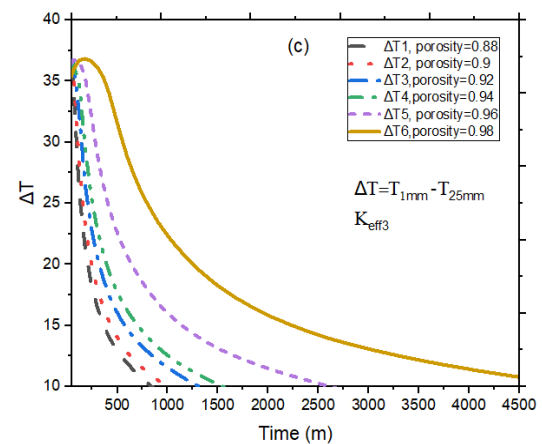
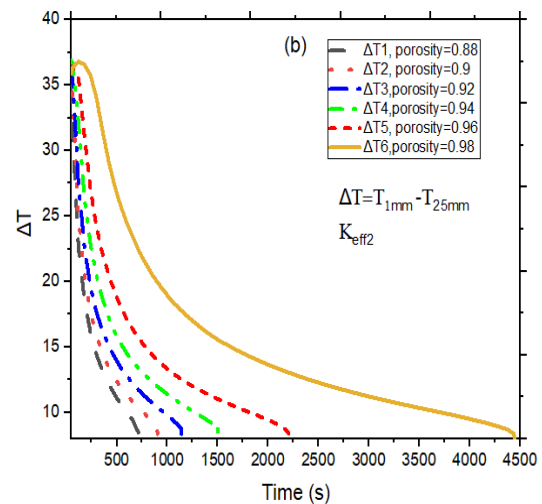
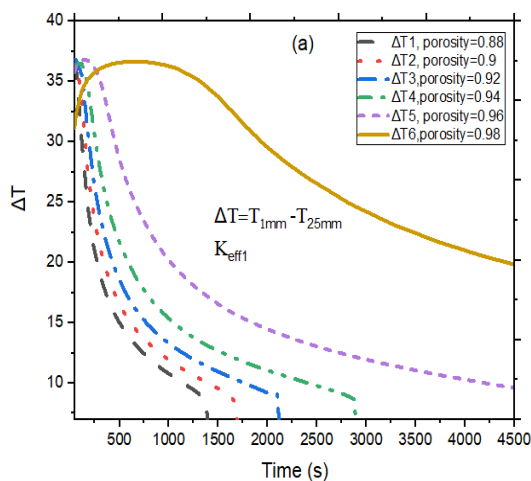


Fig. 10. Temperature differences ΔT versus time (a) by applying Boomsma and Poulikakos, Model [10](b) by applying Dai et al. Model [11], (c) and by applying Yao et al. Model [20].

5.4 Melting front position

The movement of the melting front position along the x -axis versus the time shown in Fig. 11. where the position of the melting front phase moving forward with time as expected. On the other side, it can notice an improvement in the melting front position by using metal foam/paraffin composite in comparison to the pure paraffin. Moreover, an augmentation in the position of the melting front phase observed with decreasing the porosity for instance Fig. 11 (a). exhibit the position of the melting front phase at 0.029 m after 1200 s for 0.98 porosity and the position increased gradually reaching the maximum development at 0.09 m after the 1200 s for 0.88 porosity. The mentioned behavior resembles for all used models. However, the models gave

a paradoxical recording in comparison with each other as shown in Fig. 11 (a), (b), and (c) which interpreted by the incompatible values of the effective thermal conductivity that found by models presented in this work.

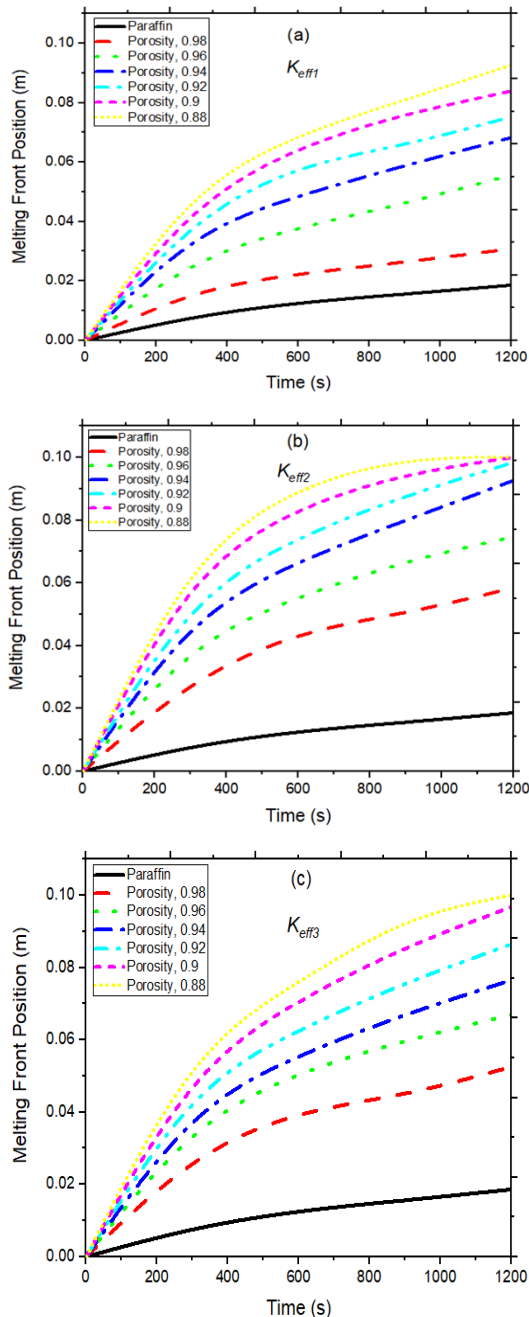


Fig. 11. Melting front position versus time (a) by applying Bomsma and Poulikakos Model [10], (b) by applying Dai *et al.* Model [11], and (c) by applying Yao *et al.* Model [20].

6. Conclusions

The thermal behavior of paraffin wax supplied to constant temperature from one side and insulated from the other side studied. The effect of Copper metal foam impregnate in the paraffin on the thermal behavior was also achieved. Using different metal foam porosities to study the effect of metal foam porosity on paraffin/metal foam composite has been indicated. Three different models based on 3D tetrakaidecahedron shape for indicating the effective thermal conductivity for paraffin/metal foam composite accomplished. It can be noticed that copper metal foam can improve the thermal conductivity of the paraffin, significantly. The porosity is proportional inversely with heat transfer rate, whenever the porosity is small, the thermal distribution along the x-axis is improved and minimizes from temperature differences. In addition, the existence of metal foam results in a rapid rising in temperatures, with the decreases in porosity. According to the mentioned, 0.88 porosity can perform an optimum behavior for the heat transfer rate, which leads to perfect thermal distribution and minimize the temperature differences. The position of the melting front phase improved with time by using copper metal foam, that less time is required to achieve the complete melting process. The minimum porosity of 0.88 recorded the maximum improvement in the position of the melting front phase. In other words, the velocity of the melting front phase augmented with minimizing the porosity. The previous data achieved by using three models and the models recorded incompatible results. The Boomsma and Poulikakos [10], indicated an impossible geometrical result, also Dai *et al.* [11] originally developed from Boomsma and Poulikakos. According to this, Yao *et al.* [20] is the most suggested model to give accurate results, for the models based on 3D tetrakaidecahedron shape. The mentioned suggestion supported by the comparison of the models with the experimental data presented by Yao *et al.* [20].

References

- 1 CHEN Z., GU M., PENG D.: Heat transfer performance analysis of a solar flat-plate collector with an integrated metal foam porous structure filled with paraffin. *Applied Thermal Engineering*, (2010), 30.14-15: 1967-1973.
- 2 VADWALA P.: *Thermal Energy Storage in Copper Foams Filled with Paraffin Wax* (Master dissertation), University of Toronto, 2011.
- 3 OZMAT B., LEYDA B., BENSON B.: Thermal applications of open-cell metal foams. *Materials and manufacturing processes*, (2004), 19.5: 839-862.
- 4 LU T., STONE H., ASHBY M.: Heat transfer in open-cell metal foams. *Acta materialia*, (1998), 46.10: 3619-3635.
- 5 SHARMA A., TYAGI V. V., CHEN C. R., BUDDHI D.: Review on thermal energy storage with phase change materials and applications. *Renewable and Sustainable energy reviews*, (2009), 13.2: 318-345.
- 6 WANG X. Q., YAP C., MUJUMDAR A. S.: A parametric study of phase change material (PCM)-based heat sinks. *International Journal of Thermal Sciences*, (2008), 47.8: 1055-1068.
- 7 POULIKAKOS D., RENKEN K.: Forced convection in a channel filled with porous medium, including the effects of flow inertia, variable porosity, and Brinkman friction. 1987.
- 8 CALMIDI, V. V., MAHAJAN, R. L.: The effective thermal conductivity of high porosity fibrous metal foams. *Journal of Heat Transfer*, (1999), 121.2.
- 9 BHATTACHARYA A., CALMIDI V. V., MAHAJAN R. L.: Thermophysical properties of high porosity metal foams. *International journal of heat and mass transfer*, (2002), 45.5: 1017-1031.
- 10 BOOMSMA K., POULIKAKOS D.: On the effective thermal conductivity of a three-dimensionally structured fluid-saturated metal foam. *International Journal of Heat and Mass Transfer*, (2001), 44.4: 827-836.
- 11 DAI Z., NAWAZ K., PARK Y. G., BOCK J., JACOBI A. M.: Correcting and extending the Boomsma–Poulikakos effective thermal conductivity model for three-dimensional, fluid-saturated metal foams. *International Communications in Heat and Mass Transfer*, (2010), 37.6: 575-580.
- 12 CALMIDI, V. V., MAHAJAN, R. L.: Forced convection in high porosity metal foams, *Journal of Heat Transfer*, (2000), 122.3: 557-565.
- 13 PHANIKUMAR M. S., MAHAJAN R. L.: Non-Darcy natural convection in high porosity metal foams. *International Journal of Heat and Mass Transfer*, (2002), 45.18: 3781-3793.
- 14 FETOUI M., ALBOUCHI F., RIGOLLET F., NASRALLAH S. B.: Highly porous metal foams: effective thermal conductivity measurement using a photothermal technique. *Journal of Porous Media*, (2009), 12.10.
- 15 XIAO X., ZHANG P., LI M.: Effective thermal conductivity of open-cell metal foams impregnated with pure paraffin for latent heat storage. *International Journal of Thermal Sciences*, (2014), 81: 94-105.
- 16 XIAO X., ZHANG P., LI M.: Preparation and thermal characterization of paraffin/metal foam composite phase change material. *Applied Energy*, (2013), 112: 1357-1366.
- 17 HAN X.H., WANG Q., PARK Y. G., T'JOEN C., SOMMERS A., JACOBI A.: A review of metal foam and metal matrix composites for heat exchangers and heat sinks. *Heat Transfer Engineering*, (2012), 33.12: 991-1009.
- 18 KAMATH P. M., BALAJI C., VENKATESHAN S. P.: Convection heat transfer from aluminium and copper foams in a vertical channel—An experimental study. *International Journal of Thermal Sciences*, (2013), 64: 1-10.
- 19 OGOH W., GROULX D.: Stefan's problem: Validation of a one-dimensional solid-liquid phase change heat transfer process. In: *Comsol Conference 2010*. 2010.

20 YAO Y., WU H., LIU Z.: A new prediction model for the effective thermal conductivity of high porosity open-cell metal foams. *International Journal of Thermal Sciences*, (2015), 97: 56-67.

21 Uddin, M. J., et al. "Numerical simulation of convective heat transport within the nanofluid filled vertical tube of plain and uneven side walls." *International Journal of Thermofluid Science and Technology* 6.1 (2019): 19060101.

22 Goud, B. Shankar, et al. "Mass Transfer Effects on MHD Flow through Porous Medium past an Exponentially Accelerated Inclined Plate with Variable Temperature and Thermal Radiation." *International journal of thermofluid science and technology* 6 (2019): 19060402.